Int. J. Electrochem. Sci., 16 **(2021)** Article ID: 21039, doi: 10.20964/2021.03.54

International Journal of
ELECTROCHEMICAL
SCIENCE
www.electrochemsci.org

Influence of Process Parameters on Electrochemical Removal of Indole: Response Surface Methodology, Mechanism and Energy Consumption

Haidong Wang[1], *Lei He*[2], *Xiaoya Chen*[2], *Kangle Gao*[1], *Bote Lu*[1], *Chunrong Wang*[2*], *Jin Cheng*[2], *Enkai Fu*[2], *Xin Hu*[2]

[1] China Metallurgical Construction Research Institute Co., Ltd., 33#, Xitucheng Road, Haidian District, Beijing 100088, PR China; wang.haidong@139.com (H.W); gaokangle@qq.com (K.G); lupotter@163.com (B.L)
[2] School of Chemical and Environmental Engineering, China University of Mining and Technology (Beijing), Ding 11#, Xueyuan Road, Haidian District, Beijing 100083, PR China;
[*]E-mail: wcrzgz@126.com

Received: 16 November 2020 / *Accepted:* 5 January 2021 / *Published:* 31 January 2021

In this study, the degradation of indole wastewater by a tin-antimony anode (Ti/SnO_2-Sb) modified by carbon nanotubes (CNTs) was evaluated in an electrochemical oxidation system. The Box-Behnken design with response surface methodology was proposed to evaluate the effects of current density, Na_2SO_4 concentration, and initial pH on the total organic carbon (TOC) removal rate. Subsequently, the process of indole degradation was optimized. Under optimal conditions (current density of 23.43 mA/cm^2, Na_2SO_4 concentration of 45.44 mmol/L, and initial pH of 9.49), the TOC removal rate reached 95.36%. Further, the electrochemical oxidation of indole at the Ti/SnO_2-Sb-CNTs anode was determined to be caused by hydroxyl and sulfate radicals using radical scavenger experiments and a mechanism analysis. The energy consumption of the electrochemical oxidation of indole was 392.74 kWh/kgTOC, and the mineralization current efficiency at 10 min was 40.40%. It would provide a reference for the engineering application of advanced treatment of industrial wastewater.

Keywords: indole; response surface methodology; mechanism; energy consumption; Ti/SnO_2-Sb-CNTs anode

1. INTRODUCTION

The demand for coke has proliferated in the wake of developments in the steel industry. In 2020, coke production will exceed 400 million tons in China[1, 2]. High-yield coke is accompanied by high-concentration coking wastewater, which is highly toxic, unstable in nature, and pollutes the environment[3]. Further, coking wastewater is difficult to biodegrade and treat. However, after anaerobic-aerobic combined treatment processes, most of its alkenes and alkynes can be degraded. Nevertheless, heterocyclic substances, such as indole and quinoline, have poor biochemical properties, and various residues remain after biochemical treatment[4-6].

As a typical nitrogen-containing heterocyclic compound in coking wastewater, indole is widely used in medicine, pesticide, and chemical industries[7-9]. When the concentration of indole is high, it has a strong fecal odor and long-lasting diffusion. Moreover, if accumulated in the body for a long period, indole, which is an enterotoxin, can cause pathological changes, such as inflammation, colon damage, and central nervous system problems[10]. In addition, indole can synergistically cause carcinogenesis. It also promotes the denitrification of secondary amines through nitrite and acts as a cancer accelerant[11]. Further, it has teratogenic and mutagenic properties. Therefore, the indole residue in coking wastewater severely restricts its safe discharge and reuse, which is of increasing public interest[12, 13]. Anodic electrochemical oxidation is a promising method for the advanced treatment of refractory organic pollutants because it has strong oxidation performance, mild treatment conditions, and environmental compatibility[14, 15]. The tin-antimony (Ti/SnO_2-Sb) anode is a representative inactive anode. As the interaction between anode surfaces is powerless, the organic matter removal rate is high, but the degree of stability is relatively poor[16].

In this study, a tin-antimony anode (Ti/SnO_2-Sb) modified by carbon nanotubes (CNTs) was employed to electrochemically oxidized indole. Moreover, the Box–Behnken design (BBD) was proposed as a response surface methodology (RSM) to evaluate the influences of current density, Na_2SO_4 concentration, and initial pH on indole and total organic carbon (TOC) removal. In addition, its operating parameters were optimized. Moreover, radical scavenger experiments were conducted, and the electrochemical oxidation mechanism was analyzed. Finally, the energy consumption and mineralization current efficiency were calculated to explore its potential economic applicability.

2. MATERIALS AND METHODS

2.1. Materials and reagents

Ti/SnO_2-Sb and Ti/SnO_2-Sb-CNTs anodes (50 mm × 50 mm × 1 mm) were prepared by our group. Methanol was of high-performance liquid chromatography (HPLC) grade, while indole, ethanol (EtOH), and tert-butanol (TBA) were of analytical grade, purchased from Sino Pharm Company. All solutions were prepared in deionized water.

2.2. Electrochemical oxidation experiment and analytical method

The Ti/SnO_2-Sb-CNTs electrode with a working area of 25 cm^2 served as the anode, while a stainless-steel plate with the same area was used as the cathode. The current density was controlled by a direct-current power supply, and the influencing factors were explored. All experiments were performed in triplicate. The pH of the solutions was adjusted using dilute H_2SO_4 and NaOH.

The concentration of indole was measured using HPLC (Ultimate 3000) with a C-18 column (250 nm × 4.6 nm × 5 nm). The detection wavelength was $\lambda = 270$ nm. Methanol and acetic acid mixtures (70:30, V/V) were employed as the mobile phase with a flow rate of 0.4 mL/min. The injection volume was 20 μL. The TOC concentration was measured using a TOC analyzer (TOC-L CPH).

2.3. RSM design

The BBD of RSM was used to explore the effects of current density (X_1), Na_2SO_4 concentration (X_2), and initial pH (X_3) on the TOC removal rate[17]. The experimental ranges and levels for the three variables are summarized in Table 1.

Table 1. Design factor codes and levels.

level factor	variable	coding level		
		-1	0	+1
Current density (mA/cm^2)	X_1	20	25	30
Na_2SO_4 concentration (mmol/L)	X_2	30	40	50
Initial pH	X_3	7	9	11

The fitting polynomial is as follows:

$$Y=\beta_0+\sum_{i=1}^{k}\beta_i X_i+\sum_{i=1}^{k}\beta_{ii} X_i^2+\sum_{\substack{i=1\\ i<j}}^{k}\beta_{ij} X_i X_j, \tag{1}$$

where Y (%) is the TOC removal rate, and β_0, β_i, β_{ii}, and β_{ij} ($i = 1, 2, 3$; $j = 1, 2, 3$; $k = 3$) are the regression coefficients.

2.4. Energy consumption calculation

Each indole molecule requires 36 electrons to be fully mineralized, which are detailed as follows:

$$C_8H_7N+16H_2O \rightarrow 8CO_2+35H^++36e^-+NH_4^+, \tag{2}$$

Therefore, the mineralization current efficiency is calculated as follows:

$$MCE = \frac{96487nV_s\Delta TOC_{exp}}{4.32\times10^7 mIt}, \tag{3}$$

where MCE (%) represents the mineralization current efficiency, V_s (L) is the volume of the solution, ΔTOC (mg/L) is the TOC change, m is the quantity of carbon atoms, I (A) is the current, t (h) is the processing time, and n is the number of transferred electrons.

3. RESULTS AND DISCUSSION

3.1. Effect of operating parameters on electrochemical oxidation process

In the Ti/SnO_2-Sb-CNTs anode electrochemical oxidation system, the removal effects of indole and TOC were related to the rate of active group generation, and conductive and hydrogen ion concentrations, which correspond to the current density, and Na_2SO_4 concentration and initial pH, respectively.

3.1.1. Effect of current density

Fig. 1a shows the degradation results of the indole concentration by current density (at 10 mA/cm^2, 15 mA/cm^2, 20 mA/cm^2, 25 mA/cm^2, and 30 mA/cm^2). As current density increased from 10mA/cm^2 to 25 mA/cm^2, the removal rate of indole increased from 82.32% to 94.83%. The generation rate of hydroxyl radicals was also determined by the current density. When the current density gradually increased, both the hydroxyl radical production and the chance of contact with indole increased, thereby accelerating the ring opening of indole molecules, which degraded them into other organic molecules, thus increasing the removal rate of indole[18]. However, when the current density was higher than 25 mA/cm^2, the removal rate decreased. The TOC removal rate also experienced a similar phenomenon (Fig. 1b). This might be because the excessive current density undermines the anode performance, limiting the electron transfer ability. This is consistent with Johanna, who also achieved lower energy and current efficiency at lower current densities[19].

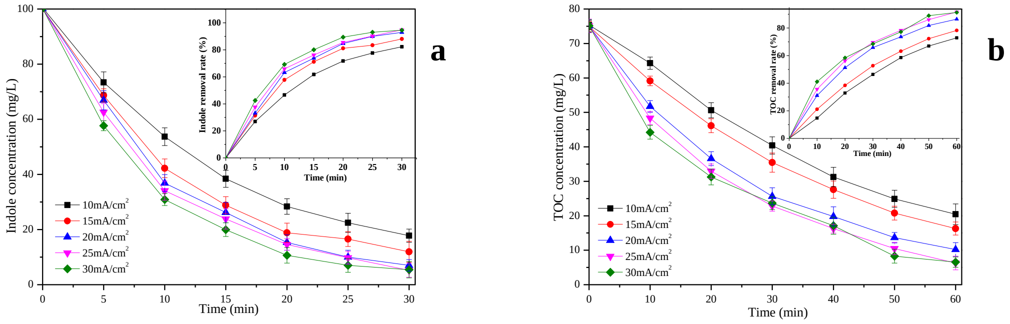

Figure 1. Effect of different current densities on (a) indole and (b) total organic carbon (TOC) removal under 30 mmol/L Na_2SO_4 concentration and an initial pH of 7.

3.1.2. Effect of electrolyte concentration

Fig. 2 shows the influence of the electrolyte concentration of Na_2SO_4 on the removal of indole and TOC. As the concentration of Na_2SO_4 increased from 10 mmol/L to 40 mmol/L, the removal rates of indole and TOC increased from 82.64% to 93.21% and 70.24% to 89.19%, respectively. However, when the Na_2SO_4 concentration increased to 50 mmol/L, both removal rates decreased (90.62%, 84.19%). Thus, the increase in Na_2SO_4 concentration may cause the solution to contain substantial electrolyte anions, cations, and indole. Moreover, various intermediate products were produced during the degradation process, which affects the mass transfer resistance to the migration of organic pollutants to the anode surface[20]. Therefore, as the concentration of organic matter continued to decrease, organic matter had to overcome a greater mass transfer resistance. Thus, it is difficult to reach the anode surface and participate in the reaction, which results in a decrease in the diffusion rate of the organic matter[21].

This result was verified by Mora-Gómez[22]. Therefore, too high of an electrolyte concentration prevents the degradation rate from improving.

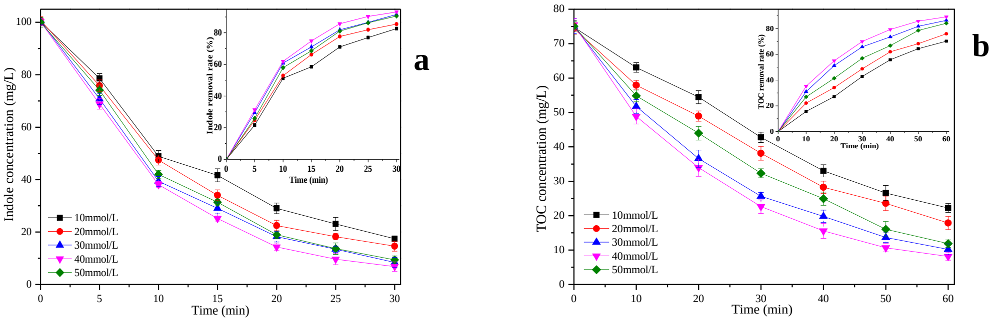

Figure 2. Effect of different Na_2SO_4 concentrations on (a) indole and (b) total organic carbon (TOC) removal under 20 mA/cm^2 current density and initial pH condition of 7.

3.1.3. Effect of initial pH

The initial pH condition influenced the electrochemical oxidation of indole and TOC, as shown in Fig. 3. Compared with acidic conditions, the degradation efficiency of indole in solution was higher under neutral or alkaline conditions. Previous research has shown that under alkaline conditions, hydroxyl radicals are adsorbed inside the positioning ion layer of the electric double layer on the anode surface[23, 24]. Meanwhile, the metal oxide anode is very hydrophilic. Therefore, H_2O and OH^- behavior in the electrochemical oxidation process changes, as shown in Eqs. (4)-(5)[25].

$H_2O\text{-}e^- \rightarrow OH^- + H^+$, (4)

$OH^-\text{-}e^- \rightarrow \cdot OH$ (under alkaline conditions). (5)

Herein, the alkaline medium was beneficial to neutralizing H^+. The stronger the alkalinity, the more likely the reaction and the more hydroxyl radicals produced, which improved the treatment effect of organic wastewater. Furthermore, Arseto et al. found that at higher pH values, the COD of the reverse osmosis concentrate (ROC) was enhanced[26]. In addition, strong acidic conditions could easily lead to the loss of metal oxides and reduce electrode life[27, 28].

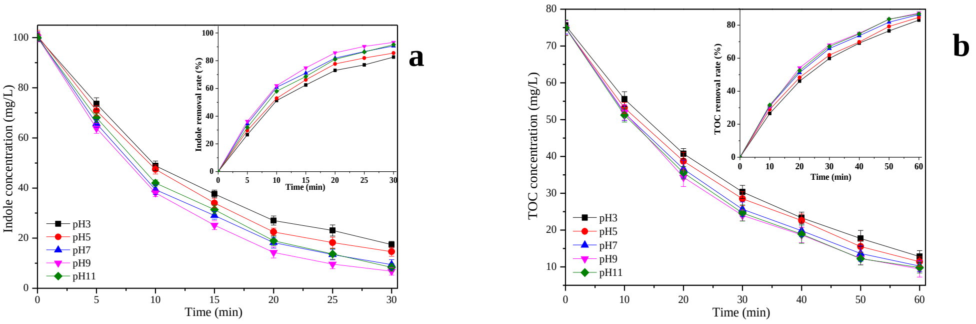

Figure 3. Effect of different initial pH values on (a) indole and (b) and total organic carbon (TOC) removal under 20 mA/cm^2 current density and 30 mmol/L Na_2SO_4 concentration condition.

3.2. Process optimization using response surface methodology

Based on the univariate factor experiments, the TOC removal rate was related to the current density, Na_2SO_4 concentration, and initial pH. Herein, it was observed that the TOC removal rate varied between 84.75% and 95.79% (Table 2).

Table 2. Test design and results

Number	Coding level			TOC removal rate / %	
	Current density mA/cm^2	Na_2SO_4 concentration mmol/L	Initial pH	Experimental value	Predicted value
1	25	40	9	95.79	95.07
2	20	40	7	89.02	88.48
3	25	40	9	95.17	95.07
4	20	50	9	92.81	93.25
5	25	50	11	93.37	93.47
6	30	30	9	86.15	85.72
7	20	40	11	92.79	92.26
8	30	40	7	85.83	86.36
9	25	30	7	89.23	89.14
10	25	40	9	94.85	95.07
11	30	50	9	86.83	86.20
12	20	30	9	87.14	87.77
13	30	40	11	84.75	85.28
14	25	40	9	94.92	95.07
15	25	30	11	91.22	91.12
16	25	50	7	92.65	92.75
17	25	40	9	94.62	95.07

The RSM analysis revealed that the model had extreme points and a range of optimal operating parameters. Therefore, the software optimization function STATISTICA was used to obtain the most optimal conditions (current density of 23.43 mA/cm^2, Na_2SO_4 concentration of 45.44 mmol/L, and initial pH of 9.49). Under these conditions, the response value of the TOC removal rate was 95.92%. To verify that the model had a good predictive effect, three sets of parallel experiments were conducted, achieving TOC removal rates of 95.85%, 95.14%, and 95.09%, with an average of 95.36%, and the relative deviation from the predicted value of 95.92% was found to be only 0.56%. This shows that using RSM to predict the optimal parameter for TOC removal had high accuracy and reliability[29].

3.3. Variance analysis and model fitting

These results prompted the use of a second-order model to describe the response of the TOC removal rate as a function of three independent factors in order to perform variance and significance analyses. The ANOVA analysis results are summarized in Table 3. The following describes the response of the TOC removal rate:

$$Y=95.07 - 2.275X_1+1.49X_2+0.675X_3-1.2475X_1X_2-1.2125X_1X_3-0.3175X_2X_3 -5.17875X_1^2-1.65875X_2^2-1.79375X_3^2. \qquad (6)$$

Table 3. ANOVA results of the quadratic polynomial regression model.

Source	Sum of squares	df	Mean square	F-value	P-value	Significance
model	224.00	9	24.89	55.37	<0.0001	Significant
A	41.40	1	41.40	92.12	<0.0001	Significant
B	17.76	1	17.76	39.51	0.0004	Significant
C	3.64	1	3.64	8.11	0.0248	Significant
AB	6.23	1	6.23	13.85	0.0074	Not significant
AC	5.88	1	5.88	13.08	0.0085	Significant
BC	0.4032	1	0.4032	0.8971	0.3751	Not significant
A^2	112.92	1	112.92	251.23	<0.0001	Significant
B^2	11.59	1	11.59	25.77	0.0014	Not significant
C^2	13.55	1	13.55	30.14	0.0009	Significant
Residual	3.15	7	0.4495			
Lack of fit	2.34	3	0.7815	3.90	0.1109	Not significant
Pure error	0.8018	4	0.2004			
Cor Total	227.15	16				

The F value was 55.37, $P < 0.0001$, indicating that the model was highly reliable, and the simulation was accurate. The lack of a fit P was 0.1109 (> 0.05), indicating that the regression effect was significant, and consequently, the model was appropriate. The correlation coefficient (R^2) was 0.9861, which is close to 1, indicating that the results were well simulated and had a small error[30].

Table 4 lists the definite correction coefficient ($R^2_{Adj,}$ 0.9683), which reveals that the response surface model analysis contributed 96.83% of the response value change. As the CV value was below 10%, the experiment was determined to be highly reliable and accurate[31, 32]. Furthermore, it was confirmed that this model could be used to explain and analyze the TOC removal rate.

Table 4. Statistical analysis of regression equation errors

Statistics project	Value	Statistics project	Value
Std. Dev.	0.67	Correlation Coefficient (R^2)	0.9861
Mean	91.01	Adjusted R^2	0.9683
CV/%	0.74	Predicted R^2	0.8293
PRESS	38.77	Adeq Precision	19.0296

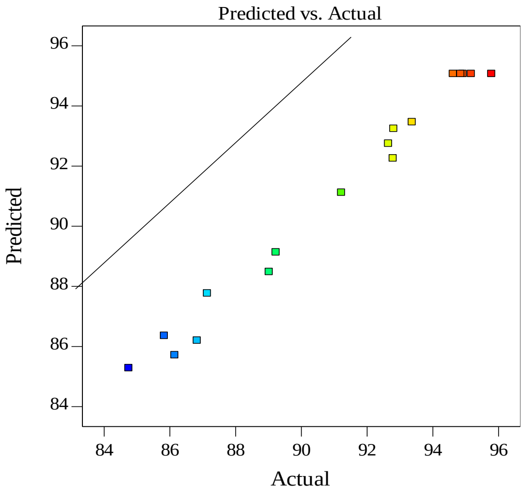

Figure 4. Experimental and predicted values of total organic carbon (TOC) removal rate.

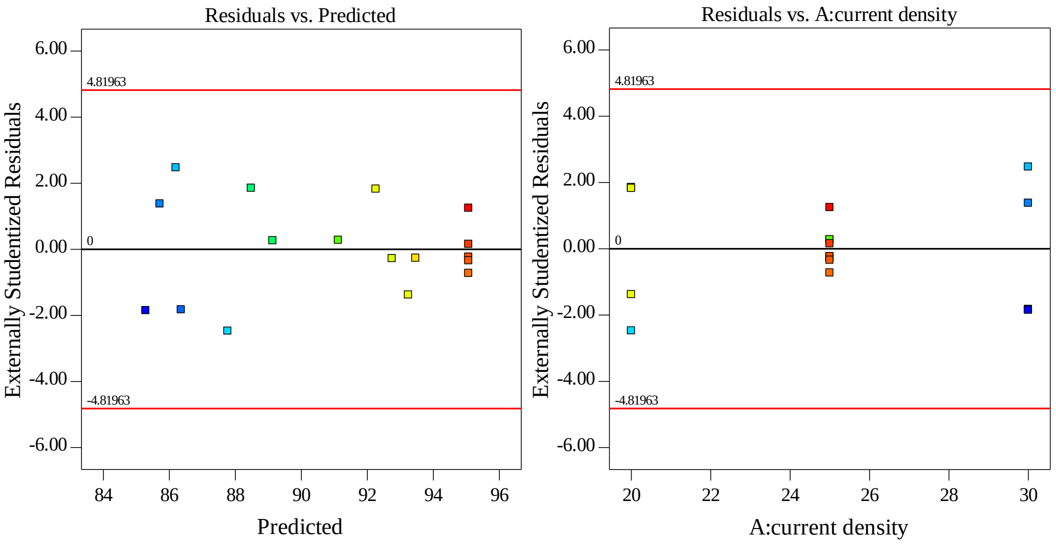

Figure 5. (a) Residual normal probability distribution diagram and (b) and residual and predicted value distribution diagram.

The relationship between the predicted and experimental values is shown in Fig. 4. The predicted values fell near the experimental data, further verifying the effectiveness of the model. The distribution of residuals and predicted values was irregular (Fig. 5), which indicated that the constructed model conformed to a normal distribution[33].

3.4. Parameters interaction impact analysis

The three-dimensional (3D) and two-dimensional (2D) contour response surfaces of the model could be expressed for the removal rate of TOC when two variables were changed while the third was kept at the zero level[34]. The interaction between current density and electrolyte concentration on the

TOC removal rate is shown in Figs. 6a and b. When the initial pH was 9, increasing the current density or Na_2SO_4 concentration improved the removal rate. In addition, when the current increased from 20 mA/cm^2 to 25 mA/cm^2 under 30 mL of Na_2SO_4 solution, the TOC removal rate increased from 87.77% to 92.06%, indicating that the electrolyte concentration had a great influence on the TOC removal rate[35]. When the initial pH was 9 and the current density was less than 25 mA/cm^2, and the removal rate of TOC was higher than 92.22% under electrolyte concentration changes in the range of 40 – 50 mmol/L. In other words, the removal rate of TOC under the appropriate current density and electrolyte concentration had a maximum value, which appeared in the range of lower current density and higher electrolyte concentration[36].

Figs. 6c and d show the interaction between the current density and initial pH and their effect on the TOC removal rate. When the pH was low, the minimum TOC removal rate was 86.36% with changing current density. Meanwhile, increasing the pH to greater than 9 and testing at the current density from 20 mA/cm^2 to 25 mA/cm^2 resulted in an increased TOC removal rate, reaching higher than 95.07%, which indicated that the TOC removal rate depended more on the change in current density than the initial pH.

Figs. 6e and f illustrate the effects of Na_2SO_4 concentration and initial pH on the removal rate of TOC with a current density of 25 mA/cm^2. The electrolyte concentration played an important role in the removal of TOC at different initial pH values. When the electrolyte concentration was equal to 30 mmol/L and the pH increased from 9 to 11, the TOC removal rate was almost unchanged, remaining in the range of 91.85% to 92.03%. Furthermore, when the pH was 7, a certain increase in the electrolyte concentration increased the TOC removal rate from 89.14% to 93.12%. Therefore, compared with pH, the influence of Na_2SO_4 concentration on TOC removal was more significant.

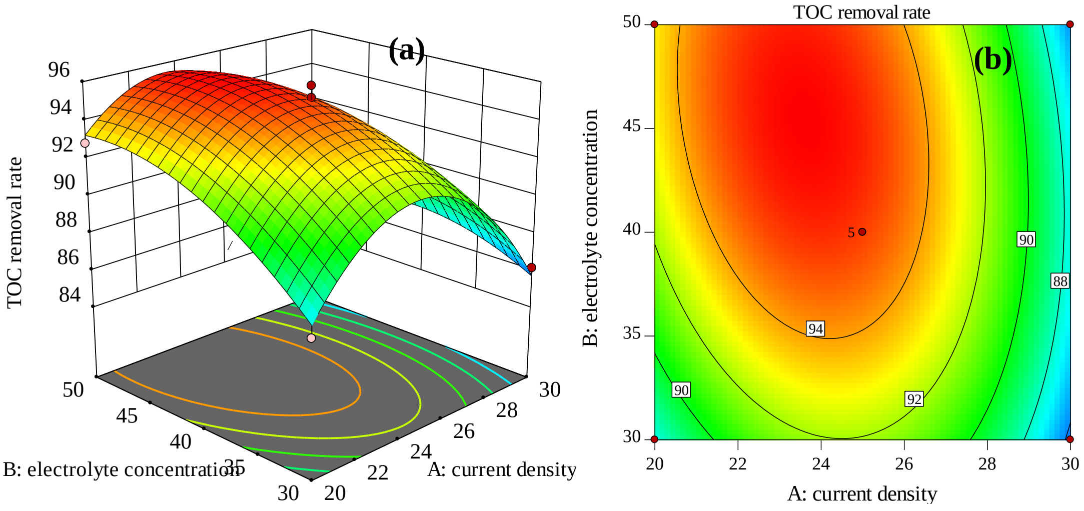

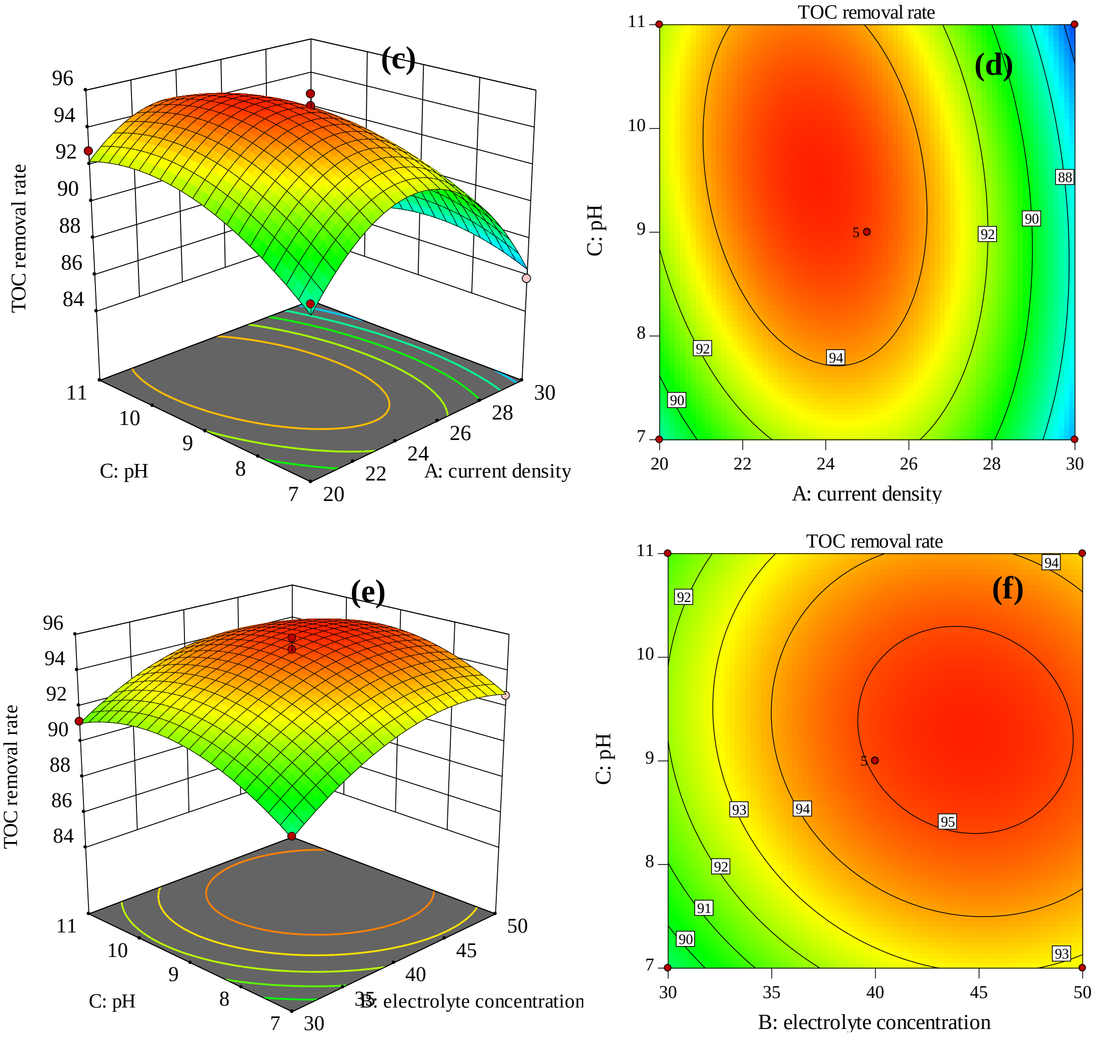

Figure 6. The two-dimensional (2D) and three-dimensional (3D) contour response surface interactions between the removal efficiency of total organic carbon (TOC) and (a – b) current density and electrolyte concentration (initial pH of 7), (c – d) current density and initial pH (electrolyte concentration of 40 mmol/L), and (e – f) electrolyte concentration and initial pH (current density of 25mA/cm^2).

3.5. Mechanism analysis of electrochemical oxidation indole

Alcohols containing α-hydrogen, such as EtOH, react quickly with hydroxyl and sulfate radicals. However, TBA, which does not contain α-hydrogen, have low reactivity with sulfate radicals because of their small reaction rate constant. Therefore, it is considered to be a special quencher for hydroxyl radicals[37, 38]. The related reaction formulas and reaction rate constants are summarized in Table 5.

By adding TBA and EtOH as radical scavengers, we determined the generation of hydroxyl and sulfate radicals and compared the indole removal rates. Further, the preliminary electrochemical degradation mechanism was analyzed. Then, we found the influence mechanism of electrochemical oxidation degradation of organic pollutants.

Table 5. Reaction formulas and constants.

Reaction formula	Reaction rate constant ($M^{-1}s^{-1}$)
$EtOH + SO_4^{\cdot -} \rightarrow$ Substance	$k_1 = 1.2 \times 10^9 - 2.8\times10^9$
$EtOH + \cdot OH \rightarrow$ Substance	$k_2 = 1.6\times10^7 - 7.7\times10^7$
$TBA + SO_4^{\cdot -} \rightarrow$ Substance	$k_3 = 3.8\times10^8 - 7.6\times10^8$
$TBA + \cdot OH \rightarrow$ Substance	$k_4 = 4\times10^5 - 9.1\times10^5$

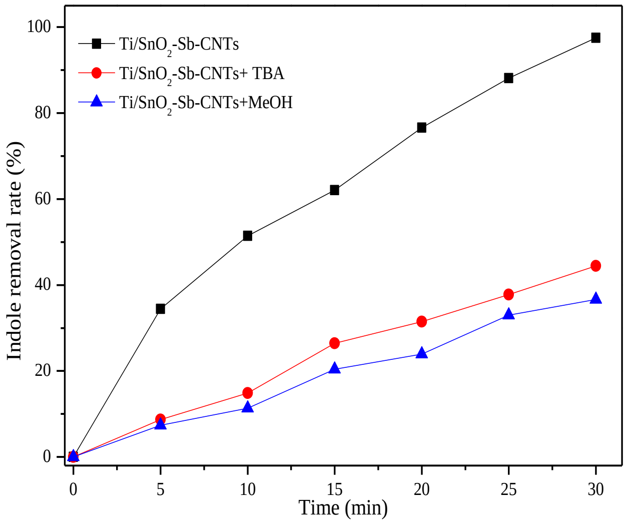

Figure 7. Effect of radical scavengers on indole degradation at 23.43 mA/cm^2 current density, 45.44 mmol/L Na_2SO_4 concentration, and initial pH of 9.49.

Fig. 7 shows the removal effect of the indole concentration with and without excessive scavengers present. Note that the effect of the control group was significantly better than that of the test group. In this study, the relative contribution rates of hydroxyl and sulfate radicals were calculated by differences in the conversion percentage. After 60 min, the indole in the control group was almost completely oxidized, and the conversion rate was 97.50%. Meanwhile, adding 0.3 mol/L of TBA, the conversion rate of indole decreased by 53.06%, proving that the TBA consumed substantial hydroxyl radicals and inhibited its oxidation reaction. After adding 0.03 mol/L of EtOH, a similar inhibitory effect was observed, however, its inhibitory effect was stronger than that of the TBA test group. The indole conversion rate was reduced by 60.87%, meaning that excessive EtOH inhibited hydroxyl radicals, whereas TBA inhibited sulfate radicals[39 40].

When an electrochemical oxidation reaction occurs, the H_2O molecules and OH^- ions in the solution lose electrons on the anode surface and generate hydroxyl radicals on the surface coating material M[41]. Herein, the surface coating material M and the O in the hydroxyl radicals did not form a common valence bond. Meanwhile, hydroxyl radicals exhibited extremely strong oxidizing properties, non-selectively oxidizing organic matter as follows[42]:

$$M+H_2O \rightarrow M\,(\cdot OH)+H^{+}+e^{-}, \qquad (7)$$

$$R+M\,(\cdot OH) \rightarrow CO_2+H_2O+H^{+}+e^{-}. \qquad (8)$$

During the reaction process, the anode also generated other active groups with strong oxidizing properties, such as sulfate radicals, as shown in Eq. (9)[43]:

$$SO_4^{2-} \rightarrow SO_4^{\cdot -}+e^{-}. \qquad (9)$$

Therefore, a reasonable mechanism analysis of the electrochemical oxidation indole was proposed (Fig. 8). Overall, the Ti/SnO_2-Sb-CNTs anode electrochemical degradation of indole was the result of the joint action of hydroxyl and sulfate radicals. Cai used a Blue-TiO_2 nanotube anode to decompose phenol, where a similar regularity was identified[44].

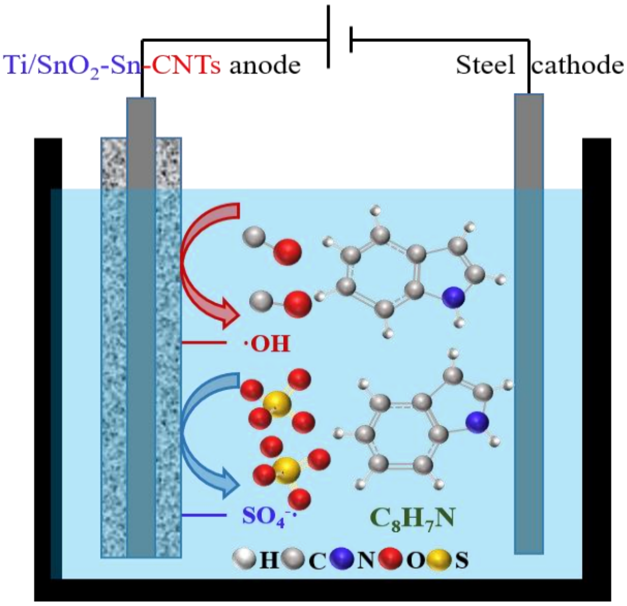

Figure 8. Reasonable preliminary degradation mechanism of indole

3.6. Energy consumption of electrochemical oxidation indole

To evaluate the cost and practicality of the Ti/SnO_2-Sb-CNTs anode, Ti/SnO_2-Sb and Ti/SnO_2-Sb-CNTs anodes were used to process indole under optimal operating parameters (Fig. 9). Then, the electrical energy consumption (EC) for 60 min and mineralized current efficiency (MCE) were determined.

In the first 30 min, the MCE of the Ti/SnO_2-Sb-CNTs anode was always greater than 20.00%, which was higher than that of the Ti/SnO_2-Sb anode. In the first 5 min, owing to the fast reaction rate and fewer intermediate products, the current utilization rate increased from 39.84% to 40.40%. As the intermediate products gradually increased, the mass transfer efficiency decreased. After 60 min, it decreased from 24.46% (5 min) to 10.79% and from 40.40% (10 min) to 12.28%. At the end of the reaction, the TOC degradation rate and the degree of MCE change were low, indicating that electrochemical oxidation did not completely convert indole into carbon dioxide, water, and other inorganic substances. Instead, it was partially converted into other forms of low molecular weight organic substances. Comparing the EC of the two anodes, they were 493.55 kWh/kgTOC (Ti-SnO_2-Sb anode) and 392.74 kWh/kgTOC (Ti-SnO_2-Sb-CNTs anode). Previous studies have ascertained that in doping CNTs, the anode has an extra-high electrocatalytic activity[45]. Herein, the oxygen evolution potential of the anode increased, thereby reducing the occurrence of the oxygen evolution reaction[46]. As its performance was improved, the degradation rate of organic matter was accelerated and the energy consumption was reduced[47]. This proved that doping carbon nanotubes reduced the anode resistance, which was similar to previous studies[48].

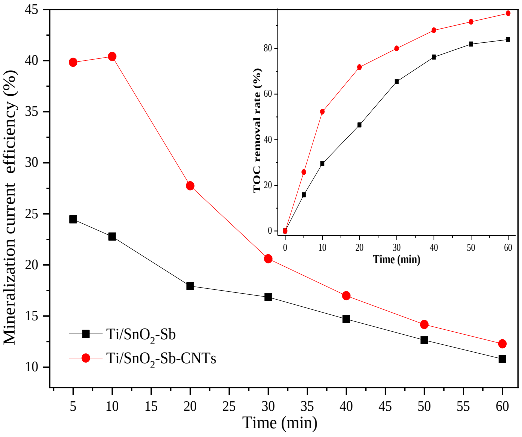

Figure 9. The transformation of total organic carbon (TOC) and mineralized current efficiency (MCE) at a 23.43 mA/cm^2 current density, 45.44 mmol/L Na_2SO_4 concentration, and an initial pH of 9.49.

4. CONCLUSIONS

The electrochemical oxidation system constituted by an Ti/SnO_2-Sb-CNTs anode rapidly degraded indole. Herein, mono-factor experiments showed that with increasing current density or electrolyte concentration, the removal rates of indole and TOC increased. Further, the interactions of current density, electrolyte concentration, and initial pH on the TOC removal rate were assessed by the RSM with BBD, and an ANOVA analysis was performed to verify the fit of the model. Under optimal conditions (current density of 23.43 mA/cm^2, electrolyte concentration of 45.44 mmol/L, and initial pH of 9.49), the TOC removal rate was 95.36%. Combined with the radical scavenger experiments, the mechanism analysis demonstrated that the degradation of indole was caused by hydroxyl and sulfate radicals. Moreover, the total energy consumption was 392.74 kWh/kgTOC, which was lower than that of the Ti/SnO_2-Sb anode, and the MCE at 10 min was 40.40%. CNTs-doped Ti/SnO_2-Sb anode can effectively improve pollutant degradation efficiency and reduce energy consumption.

ACKNOWLEDGMENTS
This research was funded by the Open Fund of the State Key Laboratory of Iron and Steel Industry Environmental Protection [No. YZC2018Ky02].

References

1. L. Mu, X. Li, X. Liu, H. Bai, L. Peng and Y. Li. *Environ. Pollut.,* 268 (2021) 115768.
2. H. Huo, Y. Lei, Q. Zhang, L. Zhao and K. He. *Energ. Policy,* 51 (2012) 397.
3. W. Zhao, Q. Sui and X. Huang. *Sci. Total Environ.,* 635 (2018) 716.
4. Q. Ma, Y. Qu, W. Shen, Z. Zhang, J. Wang and Z. Liu. *Bioresour. Technol.,* 179 (2015) 436.
5. K. Yuan, S. Li and F. Zhong. *J. Hazard. Mater.,* 400 (2020) 123117.
6. Y. Cui, W. Kang, L. Qin, J. Ma, X. Liu and Y. Yang. *Chem. Eng. J.,* 397(2020) 125480.
7. S.C. Kim and F.E. Massoth. *Ind. Eng. Chem. Res.,* 39 (2000) 1705.
8. C. Chitra, D.S. Franklin, S. Sudarsan, S. Sakthivel and S. Guhanathan. *Int. J. Biol. Macromol.,* 95 (2017) 363.
9. Y. Ji, Y. Hou, S. Ren and W. Wu. *Sep. Purif. Technol.,* 258 (2021) 117997.
10. L.C. Almeida, R.D. Correia, A. Marta, G. Squillaci, A. Morana and F.L. Cara. *Appl. Surf. Sci.,* 480 (2019) 979.
11. J. Wang, M. Wang, K. Chen, S. Zha, C. Song and J. Zhu. *Org. Lett.,* 18 (2016) 1178.
12. S. Abouzeid, U. Beutling, F. Surup, B. F.M. Abdel, M.M. Amer and F. A Badria. *J. Nat. Prod.,* 80 (2017) 2905.
13. H. Zhu, W. Ma, H. Han, C. Xu, Y. Han and W. Ma. *Chemosphere,* 209 (2018) 319.
14. S. Chai, Y. Wang, Y. Zhang, M. Liu, Y. Wang and G.H. Zhao. *Environ. Sci. Technol.,* 51 (2017) 8067.
15. N,E. Pica, J. Funkhouser, Y. Yin, Z. Zhang, D.M. Ceres and T. Tong. *Environ. Sci. Technol.,* 53 (2019) 12602.
16. Q. Bi, W. Guan, Y. Gao, Y. Cui, S. Ma and J .Xue. *Electrochim. Acta,* 306 (2019) 667.
17. S.L.C. Ferreira, R.E. Bruns, H.S. Ferreira, G.D. Matos, J.M. David and G.C. Brandão. Anal. *Chim. Acta,* 597 (2007) 179.
18. Q. Zhang, W. Huang, J.M. Hong and B.Y. Chen. *Chem. Eng. J.,* 343 (2018) 662.
19. J. Zambrano and B. Min. *Environ. Technol. Innov.,* 18 (2020) 100632.
20. S.J. Min, J.G. Kim and K. Baek. *J. Hazard. Mater.,* 400 (2020) 123083.
21. J.D. Milshtein, K.M. Tenny, J.L. Barton, J. Drake and R.M. Darling. J. *Electrochem. Soc.,* 164 (2017) E3265.
22. J. Mora-Gómez, M. García-Gabaldón, J. Carrillo-Abad, M.T. Montañés, S. Mestre and V. Pérez-Herranz. *Sep. Purif. Technol.,* 241(2020) 116684.
23. A.J. Feitz and T.D. Waite. *Environ. Sci. Technol.,* 37 (2003) 561.
24. J. Mendret, M. Hatat-Fraile, M. Rivallin and S. Brosillon. *Sep. Purif. Technol.,* 118 (2013) 406.
25. E.B. Monroe and M.L. Heien. *Anal. Chem.,* 85 (2013) 6185.
26. A.Y. Bagastyo, D.J. Batstone, I. Kristiana, W. Gernjak, C. Joll and J. Radjenovic. *Water Res.,* 46 (2012) 6104.
27. C. Picioreanu, M.C.M. Van Loosdrecht, T.P. Curtis and K. Scott. *Bioelectrochemistry,* 78 (2010) 8.
28. L. Ibing, T. Gallasch, A. Friesen, P. Niehoff, A. Hintennach and M. Winter. J. *Power Sources,* 475 (2020) 1.
29. C.R.T. Tarley, G. Silveira, W.N.L. Dos Santos, G.D. Matos, E.G.P. Da Silva and M.A. Bezerra. *Microchem. J.,* 92 (2009) 58.
30. S. Karimifard and M.R. Alavi Moghaddam. *Sci. Total Environ.,* 640 (2018) 772.
31. J.P. Wang, Y.Z. Chen, Y. Wang, S.J. Yuan and H.Q. Yu. *Water Res.,* 45 (2011) 5633.

32. S. Popović, M. Karadžić and J. Cakl. *J. Clean. Prod.*, 231 (2019) 320.
33. R. Hazime, Q.H. Nguyen, C. Ferronato, T.K.X. Huynh, F. Jaber and J.M. Chovelon. *Appl. Catal. B Environ.*, 132 (2013) 519.
34. Y. Zhang, H.,Wei Q. Xin, M. Wang, Q. Wang and Q .Wang. J. *Environ. Manage.*, 183 (2016) 726.
35. S. Salam, T. Choudhary, A. Pugazhendhi, T.N. Verma and A. Sharma. *Fuel*, 279 (2020) 118469.
36. H. Abou Oualid, Y. Abdellaoui, M. Laabd, M. El Ouardi, Y. Brahmi and M. Iazza. *ACS Omega.*, 5 (2020) 22192.
37. Y. Zhang, J.W.C. Wong, P. Liu and M. Yuan. *J. Hazard. Mater.*, 191(2011) 136.
38. S. Zhang, V. Rouge, L. Gutierrez and J.P. Croue. *Water Res.*, 163 (2019) 114846.
39. Y. Wang, M. Chen, C. Wang, X. Meng, W. Zhang and Z. Chen . *Chem. Eng. J.*, 374 (2019) 626.
40. H. Hai, X. Xing, S. Li, S. Xia and J. Xia. *Sci. Total Environ.*, 738 (2020) 1.
41. C. Bruguera-Casamada, I. Sirés, E. Brillas and R.M. Araujo. *Sep. Purif. Technol.*, 178 (2017) 224.
42. Y. Zhang, J. Li, J. Bai, X. Li, Z. Shen and L. Xia. *Appl. Catal. B Environ.*, 238 (2018) 168.
43. A. Farhat, J. Keller, S. Tait and J. Radjenovic. *Environ. Sci. Technol.*, 49 (2015) 14326.
44. J. Cai, M. Zhou, Y. Pan, X. Du and X. Lu. *Appl. Catal. B Environ.*, 257 (2019) 117902.
45. C.J. Yang, Q.F Shen, D.C. Zhai and Y. Gu. *J. Appl. Electrochem.*, 49 (2019) 67.
46. T. Wu, G. Zhao, Y. Lei and P. Li. *J. Phys. Chem. C,* 115 (2011) 3888.
47. Y. He, W. Huang, R. Chen, W. Zhang, H. Lin and H. Li. *Sep. Purif. Technol.*, 156 (2015) 124.
48. P. Duan, S. Gao, J. Lei, X. Li and X. Hu. *Environ. Pollut.*, 263 (2020) 114436.